RESEARCH ARTICLE

Open Access

Remotely mind-controlled metasurface via brainwaves

Ruichao Zhu[1], Jiafu Wang[1*] ⓘ, Tianshuo Qiu[1], Yajuan Han[1], Xinmin Fu[1], Yuzhi Shi[2], Xingsi Liu[3], Tonghao Liu[1], Zhongtao Zhang[1], Zuntian Chu[1], Cheng-Wei Qiu[3*] and Shaobo Qu[1*]

Abstract

The power of controlling objects with mind has captivated a popular fascination to human beings. One possible path is to employ brain signal collecting technologies together with emerging programmable metasurfaces (PM), whose functions or operating modes can be switched or customized via on-site programming or pre-defined software. Nevertheless, most of existing PMs are wire-connected to users, manually-controlled and not real-time. Here, we propose the concept of remotely mind-controlled metasurface (RMCM) via brainwaves. Rather than DC voltage from power supply or AC voltages from signal generators, the metasurface is controlled by brainwaves collected in real time and transmitted wirelessly from the user. As an example, we demonstrated a RMCM whose scattering pattern can be altered dynamically according to the user's brain waves via Bluetooth. The attention intensity information is extracted as the control signal and a mapping between attention intensity and scattering pattern of the metasurface is established. With such a framework, we experimentally demonstrated and verified a prototype of such metasurface system which can be remotely controlled by the user to modify its scattering pattern. This work paves a new way to intelligent metasurfaces and may find applications in health monitoring, 5G/6G communications, smart sensors, etc.

Keywords: Brainwave, Mind-controlled, Reprogrammable metasurface, Intelligent metasurface

1 Introduction

Metamaterials, which are composed of periodic or quasi-periodic sub-wavelength structures (called as meta-atoms), have attracted extensive attention from the fields of optics, electronics, physics, materials and others, due to their extraordinary physical properties [1–3]. The advent of metamaterials provides a new concept of designing artificial materials, bringing vigor and vitality to advanced functional materials [4, 5]. Metasurface, as the two-dimensional counterpart of metamaterial, usually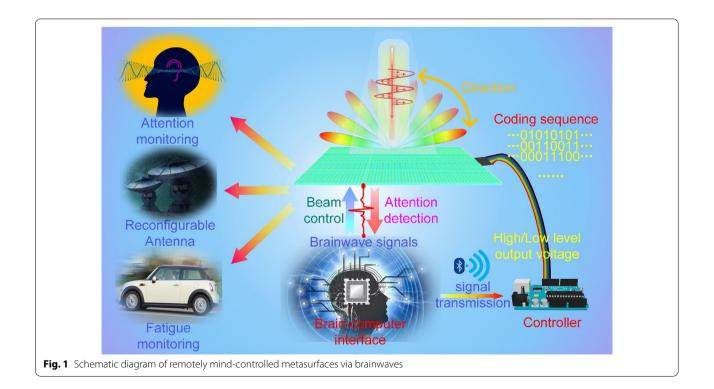 refers to planar arrays of meta-atoms arranged in two dimensional (2D) manners [6, 7]. The meta-atoms can modulate nearly all the characteristics of electromagnetic (EM) waves, such as amplitude, phase, polarization and modes, metasurfaces have provided unprecedented degree of freedom (DOF) in manipulating EM waves. A large variety of functional metasurfaces have been presented [8, 9]. In particular, metasurface-based multidimensional light manipulation attracts more and more attention due to the increasing demand for more integrated and compact devices [10–12]. Typically, integration of multiple functions can be realized by aperture multiplexing in space domain, such as meta-atom combination [13], polarization multiplexing through anisotropic meta-atoms [14] and wavelength multiplexing via dispersion [15] and others. For these metasurfaces, the functions are predefined and cannot be altered. Therefore, they can be called static metasurfaces. Due to the passive nature of static metasurfaces, the integrated multiple functions are limited and are usually contradictory

*Correspondence: wangjiafu1981@126.com; chengwei.qiu@nus.edu.sg; qushaobo@126.com

[1] Shaanxi Key Laboratory of Artificially-Structured Functional Materials and Devices, Air Force Engineering University, Xi'an 710051, Shaanxi, China

[3] Department of Electrical and Computer Engineering, Faculty of Engineering, National University of Singapore, 4 Engineering Drive 3, Singapore 117583, Singapore

Full list of author information is available at the end of the article

to one another. This necessitates the actively-controlled dynamic metasurfaces, whose functions can be altered or customized according to specific scenarios. Many control manners, such as optical switch, electric biasing, mechanical rotation or displacement, free carrier effect, microfluidic and temperature-induced phase variation, have been applied to dynamic metasurfaces [16–27]. With these control manners, time-domain DOF is introduced into metasurfaces, and multifunctional metasurfaces can be greatly enriched via time–space control.

Since the EM responses of meta-atoms can be altered fast and conveniently using voltage biasing, electric control is the most common manners of achieving dynamic metasurfaces, i.e. embedding diodes, varactors and the like within meta-atoms, applying DC voltages to change the effective electrical parameters and thus adjusting responses of meta-atoms upon incident EM waves. On the basis of the electric control manner, the concept of coding metasurface was proposed, in which the responses of meta-atoms can be represented by '0' or '1' [28]. Later, the concept of digital metasurface was further put forward, which bridges the gap between analog responses and digital characterizations of metasurfaces. PIN diodes are commonly used to switch among different functions corresponding to different coding sequences. Moreover, the state of '0' and '1' can also represent high and low levels in digital circuits, which means that the coding sequences can be controlled by Field-Programmable

Gate Array (FPGA) [28–32]. Using electronic components and FPGA, programmable metasurfaces (PMs) with multiple or switchable functions can be realized through on-site programming. Further integrated with sensors and driven by pre-defined software, self-adaptive PMs can be realized for a specific scenario [33–35]. The self-adaptability significantly improves the response rate by removing human involvement. Nevertheless, for these PMs, switches among different functions generally rely on manual operation when the application scenarios are changed, either by on-site reprogramming or by re-defining the driven software. The fundamental framework is actually wire-connected, manually-controlled and non-real-time switched, which levels down their glamour of intellectualization. Therefore, it is fascinating to construct a fundamental framework that can realize remote, wireless, real-time, mind-controlled functional metasurfaces. Moreover, as the initiator, executor or user of metasurfaces, the involvement and participation of human is usually necessary in many scenarios and it is better for human to directly control the metasurface with their mind. As is well-known, human's brain will generate brainwaves in the process of thinking. If we can collect brainwaves and use them as the control signals of metasurfaces, we can not only allow the users to control metasurfaces with their mind, but also can improve the response rate of metasurfaces. This will make a big step towards truly intelligent metasurfaces. Figure 1

Fig. 1 Schematic diagram of remotely mind-controlled metasurfaces via brainwaves

exhibits the schematic diagram of the mind-controlled metasurfaces, which describes the main flow and design ideas of this work.

In this paper, we propose a framework of realizing remotely mind-controlled metasurface (RMCM) using brainwave extraction module. This framework consists of three parts, i.e. sensor, controller and actuator. The sensor refers to the brainwave module that can record brainwaves and transmit them to the controller via Bluetooth. The controller consists of microprogrammed control unit (MCU) and output terminal. Arduino is selected as the controller in this work. The controller receives brainwave signals from the sensor, converts them into attention signals and then feed the attention signals into the actuator. According to the level of attention intensity, the attention signals fall within four separate intervals which are characterized by four thresholds. The output pins of the controller are connected to the actuator, and the high/low level of output voltage corresponds to the coding 1/0 sequence. The actuator is a PM with PIN diodes embedded within its meta-atoms. Under the switch on/off state of the PIN diodes, a phase difference of 180° will be produced to enable 1-bit coding. The output voltage level sequences from the controller denote different coding sequences on the metasurface, so as to control the scattering pattern. A prototype was fabricated and tested. The test results verify the mind controllability of such a metasurface. Different from the traditional dynamic metasurface, this metasurface could manipulate the EM wave through the real-time response of the human brain, rather than manual operation. Our design maps the thinking of the human brain into metasurface EM modulation, which effectively increases the rate of EM modulation. This work paves a new way to intelligent metasurfaces and may find applications in health monitoring, 5G/6G communications, smart sensors, etc.
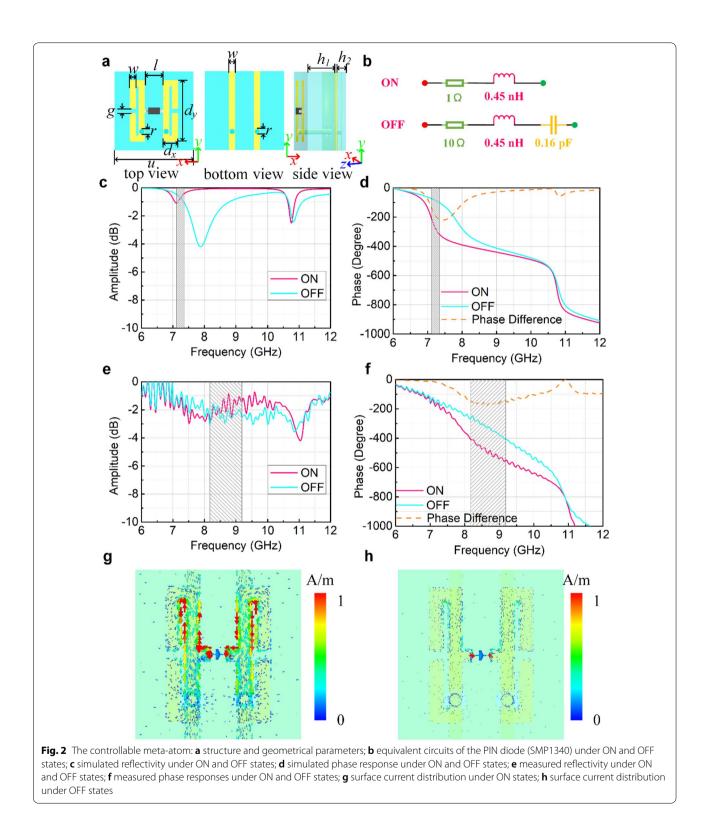
2 Controllable meta-atom design

The details and EM responses of the controllable meta-atom are shown in Fig. 2. The geometrical parameters and structure pattern are given in Fig. 2a. The double-C-shape structure, with one PIN diode embedded in between, is adopted as the unit structure to enable electrical control. The meta-atom comprises three metallic layers, the top unit structure layer, the middle ground layer and the bottom biasing layer. The top and bottom layers are connected by metallized vias. Geometrical dimensions of the meta-atom are as follows. The repeating period $u = 9$ mm. The width and length of C-shape structure $d_x = 1.7$ mm, $d_y = 7$ mm. The gap width $g = 0.5$ mm. The strip width $w = 0.7$ mm. The width of biasing lines on the bottom is also $w = 0.7$ mm. The distance between the two C-shape patterns is $l = 2.1$ mm.

The diameter of metallized vias is $r = 0.6$ mm. The thickness of all the metallic part is 0.017 mm. Two dielectric substrate layers separate the three metallic layers and here we adopt a commercial microwave laminate F4B substrate with a dielectric constant $2.65(1 + 0.001j)$. The thicknesses of the two dielectric substrate layers are $h_1 = 3.5$ mm and $h_2 = 1$ mm.
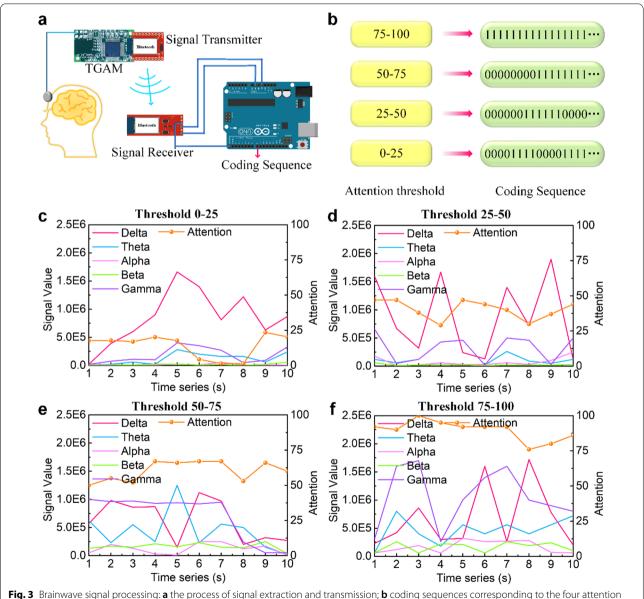
The PIN diode is embedded in between the two C-shape structures. SMP1340-011 PIN diodes are used and the equivalent circuit is shown in Fig. 2b, [36–38]. As shown in Fig. 2b, the ON and OFF state of the PIN diode can be described by RL and RLC circuits, respectively. The meta-atom under ON and OFF states was simulated using the field-circuit co-simulation method. The simulations were conducted using the commercial software CST Microwave Studio. The simulated EM responses under ON and OFF states are plotted in Fig. 2c and d. The reflectivity is higher than 80% under the two states and a phase difference $180° \pm 37°$ is achieved within 7.12–7.35 GHz. In practice, the SMP1340 PIN diode will have different sub-models for different package configurations, which will make the parameters of its equivalent circuits a bit different. In order to obtain the accurate equivalent circuit model, a metasurface prototype was fabricated and measured. The measured EM responses are shown in Fig. 2e and f. The measured results show that the reflectivity is about − 2 dB (64%) under ON and OFF states and the phase difference is $180° \pm 37°$ is achieved in 8.17–9.19 GHz. Here, the inconsistencies between the measured EM responses and simulated EM responses are existed, which are caused by machining error. And the equivalent circuit of simulation is not completely equivalent to the working mode of the actual circuit. Therefore, the equivalent circuit of simulation is modified to further simulate the actual situation. The measurement setup and the updated equivalent circuits are given in the Additional file 1: Note S1. In order to better understanding of the phase modulation, we monitor the surface current distribution of the structure between ON and OFF states in Fig. 2g and h. When the diode state is 'ON', surface current flows between the two 'C' pattern. On the contrary, when the diode state is 'OFF', surface current is very weak. The surface current distribution explicitly illustrates the reason of phase modulation. Therefore, the meta-atom can be used to enable 0−1 coding within 8.17–9.19 GHz.
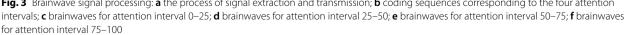
3 Signal extraction and wireless transmission of brainwaves

In the process of thinking, brains will produce brainwaves in the form of bioelectric signals. Usually, dry or wet electrodes can be used to record the fluctuation of bioelectric currents. Herein, we use ThinkGear AM (TGAM)

Fig. 2 The controllable meta-atom: **a** structure and geometrical parameters; **b** equivalent circuits of the PIN diode (SMP1340) under ON and OFF states; **c** simulated reflectivity under ON and OFF states; **d** simulated phase response under ON and OFF states; **e** measured reflectivity under ON and OFF states; **f** measured phase responses under ON and OFF states; **g** surface current distribution under ON states; **h** surface current distribution under OFF states

module to extract brainwave signals. The TGAM module mainly includes TGAT chip from NeuroSky, a highly integrated single chip electroencephalo-graph (EEG)

sensor, and it supports dry electrode detection for collecting EEG signals. Moreover, the TGAM module integrates EEG signal extraction and conversion algorithms

that can extract attention information from brainwaves. Commonly, attention level is reflected in multiple waves working together and the relationship between those waves and attention level is complicated. Fortunately, the TGAM module integrate built-in algorithms for obtaining the attention level by the multiple waves. The Attention Meter algorithm indicates the intensity of attention by a value within [0, 100]. The value of attention intensity is extracted and transmitted via bluetooth. The bluetooth of TGAM is set to be slave mode and the bluetooth connected to Arduino is set to be master mode. The baud

rate of signal transmission is 57600 bit/s. Subsequently, the value of attention intensity can be sent to Arduino. Arduino, as the controller, receives and processes the brainwave signals. The wireless transmission process is illustrated in Fig. 3a. The attention value is reported on a relative scale from 0 to 100. On this scale, the attention intensity is divided into four threshold intervals, namely, 0–25, 25–50, 50–75 and 75–100. When the user focuses on a single idea, the attention level will increase; when the user is distracted, the attention level will decrease. Therefore, the four threshold intervals correspond to

Fig. 3 Brainwave signal processing: **a** the process of signal extraction and transmission; **b** coding sequences corresponding to the four attention intervals; **c** brainwaves for attention interval 0–25; **d** brainwaves for attention interval 25–50; **e** brainwaves for attention interval 50–75; **f** brainwaves for attention interval 75–100

distracted, neutral, concentrated and extremely concentrated attention intensity, respectively. Different intervals correspond to different output pin levels and thus to different coding sequences. Under different coding sequences, different scattering patterns can be achieved. The intervals of 0–25, 25–50, 50–75 and 75–100 correspond to the coding unit with 4, 6, 8 and all meta-atoms, respectively. The corresponding coding sequences are depicted in Fig. 3b. TGAM can effectively extract brainwave signals and convert them to attention intensity information through its built-in conversion algorithm. Delta, theta, alpha, beta, gamma waves which represent the different frequencies of brainwave activity are extracted and converted to attention intensity. The corresponding frequency of delta, theta, alpha, beta, gamma is 0–4 Hz, 4–8 Hz, 8–13 Hz, 13–30 Hz, 30–100 Hz, respectively [39, 40]. The users alter their attention concentration through their thoughts, and keep it within a interval as much as possible. The switch among different states are realized through brainwave control and maintain the interval for 10 s with brain power. According to development document, the feedback time of TGAM module is about 78 ms, which is almost instantaneous. Here, sampling time of MCU is set to 1 s. The variations of brainwaves and shifts of attention intensity were recorded and are plotted in Fig. 3c–f, from which it can be found that the user can effectively alter the attention intensity and maintain it within a certain intensity interval, although the signals may be disturbed by minor fluctuations. Moreover, the brainwave module is commercial and is applicable for most common people. Therefore, the mind-control method by brainwaves is robust for achieving metasurface control.

4 Scattering pattern control

When plane waves impinge on a reflective coding metasurface, the far-field scattering pattern can be expressed as [28, 41, 42]:

$$F(\theta, \varphi) = f_{m,n}(\theta, \varphi) S_a(\theta, \varphi) \tag{1}$$

where θ and ϕ represent the elevation and azimuth angles, respectively; $f_{m,n}(\theta, \phi)$ is the scattering pattern function of the coding unit and can be considered as a constant due to the sub-wavelength size of meta-atoms. $S_a(\theta, \phi)$ is the array factor, which can be expressed as

$$S_a(\theta, \varphi) = \sum_{m=1}^{M} \sum_{n=1}^{N} \exp\left\{ j[\varphi_{m,n} + k_0 D_x(m - 1/2)(\sin\theta\cos\varphi - \sin\theta_i\cos\varphi_i) \right.$$
$$\left. + k_0 D_y(n - 1/2)(\sin\theta\sin\varphi - \sin\theta_i\sin\varphi_i)] \right\} \tag{2}$$

where k_0 is the wave vector of EM waves in free space, M and N the number of units in x and y directions, $\phi_{m,n}$ the phase response of coding elements at position (m,n). D_x and D_y are the sizes of elements in x and y directions. θ_i represents the incident angle and here we consider the scattering pattern under normal incidence, that is, $\theta_i = 0°$. Then, the far-field scattering pattern can be simplified as
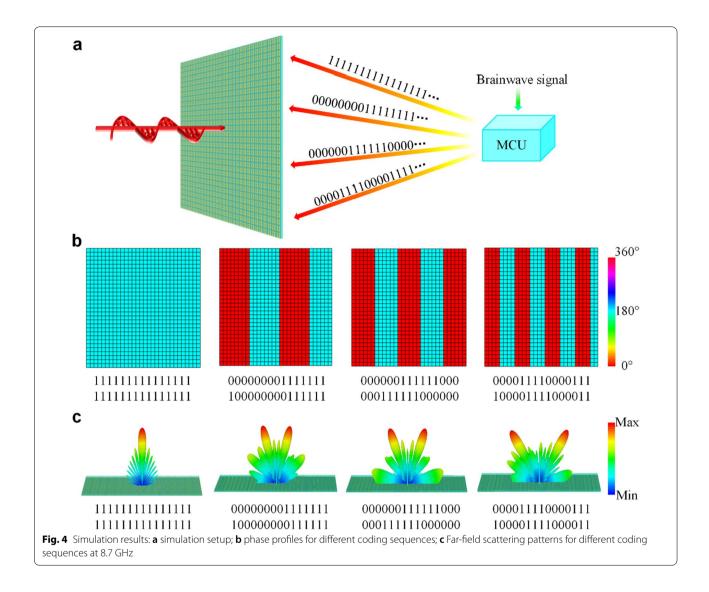
$$F(\theta, \phi) = C \sum_{m=1}^{M} \sum_{n=1}^{N} \exp\{j[\varphi_{m,n} + k_0 D_x(m - 1/2)(\sin\theta\cos\varphi)$$
$$+ k_0 D_y(n - 1/2)(\sin\theta\sin\varphi)]\} \tag{3}$$

According to Eq. (3), when the coding sequence is changed, the length of D_x will be changed, and correspondingly the far-field scattering pattern will also be changed. The scattered beam will be split for non-uniform coding sequences and the split angle is depedent on the length of coding element D_x. The longer the coding element, the smaller the split angle. Considering the mapping between the scattering patterns and the four attention intensity intervals, it can be concluded that the intenser the attention, the more concentrated the metasurface's scattering pattern.

Using brainwave signals sent to MCU as the control signal, the coding sequences on the metasurface can be altered according to the user's attention intensity, as schematically illustrated in Fig. 4a. In this way, the scattering pattern of the metasurface can be controlled remotely via the user's mind. Furthermore, according to different coding sequences in Fig. 4b, full-wave simulations were carried out to verify the metasurface. The phase profiles corresponding to these coding sequences are shown in Fig. 4c, from which variation of coding length can be seen directly. The simulation setups are as follows. The metasurface is placed on *XOY* plane and *x*-polarized plane waves are normally incident upon the metasurface from $+Z$ direction. The boundaries along x, y and z directions are set as open add space. Far-field monitor is set at 8.7 GHz to get the far-field scattering pattern. The simulated far-field results are shown in Fig. 3d, in which different coding sequences correspond to different far-field scattering patterns. As predicted, the higher the attention value, the more concertrated the scattering patterns and the smaller the split angle.

Fig. 4 Simulation results: **a** simulation setup; **b** phase profiles for different coding sequences; **c** Far-field scattering patterns for different coding sequences at 8.7 GHz
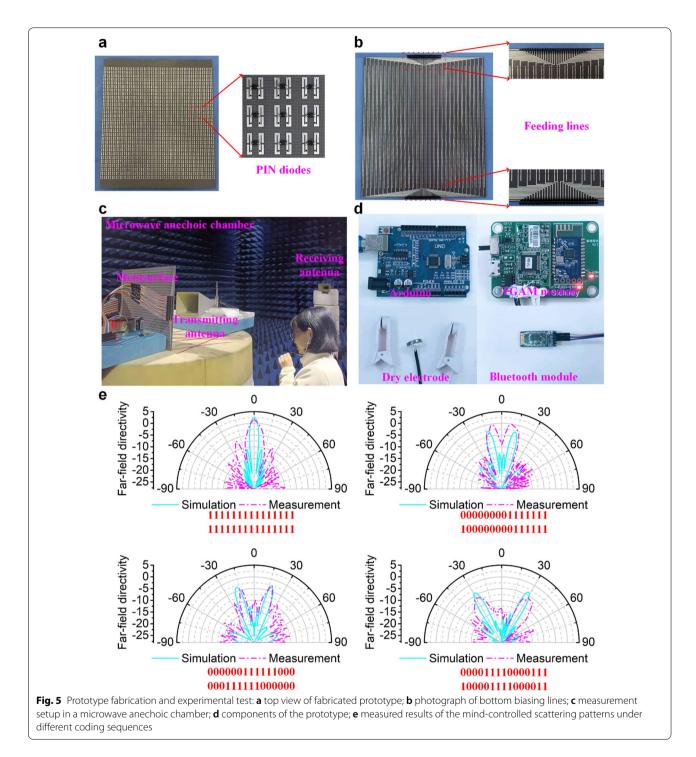
5 Experimental test

In order to further verify the design framework, a RMCM prototype was fabricated and tested. The metasurface was fabricated using conventional Printed Circuit Board (PCB) techniques. PIN diodes with SOD-323 packaging were soldered on the metasurface, as shown by the inset in Fig. 5a. Photograph of the bottom biasing lines is given in Fig. 5b and the arrangement of biasing lines is supplemented in the Additional file 1: Note S2. Fig. 5d shows the components of the RMCM, including the metasurface-control module, brainwave extraction module, Bluetooth wireless transmission module, DC power supply module, single chip microcomputer module and other auxiliary wirings. The brainwave signal acquisition module is a commercial brainwave sensor module, with dry electrodes as the signal acquisition equipment, which facilitates practical applications. The wearing mode of brainwave signal acquisition equipment is supplemented in Additional file 1: Note S3. The user wears the dry electrodes, which collect and then send brainwaves wirelessly towards the RMCM. Upon the incoming brainwaves, the RMCM will respond by changing its scattering pattern. In this way, the metasurface can be remotely controlled by the user's mind.

The prototype was measured in an anechoic chamber, as is shown in Fig. 5c. The metasurface, together with the controller, is placed on the turntable mount. The controller we adopted here is Arduino UNO R3, through which the user can freely control the current state through TGAM module. The output pins of Arduino are connected to the biasing lines of the metasurface, so as to control each meta-atom at their respective designated positions on the metasurface. The transmitting antenna is placed along the normal of

Fig. 5 Prototype fabrication and experimental test: **a** top view of fabricated prototype; **b** photograph of bottom biasing lines; **c** measurement setup in a microwave anechoic chamber; **d** components of the prototype; **e** measured results of the mind-controlled scattering patterns under different coding sequences

the metasurface while the receiving antenna can rotate around the metasurface, so as to measure the scattering patterns under normal incidence. Far-field scattering patterns are measured for different coding sequences. In order to directly observe the mind-controllability of coding sequence, an LED array is used to visually

display the coding state. The circuit component is supplemented in Additional file 1: Note S4.

The measured scattering patterns of the RMCM prototype are plotted in Fig. 5e, in which the simulated results are also plotted for the sake of comparison. The pattern in Fig. 5e is the normalized RCS which is normalized by an

equal size metal plate. And there are still little differences between them, which are caused by simulation error and machine error. The diode is simulated by the equivalent circuit model, which only approximate the actual situation and cannot completely simulate the actual situation. Meanwhile, the diode welding also has certain deviation and the size effect of the diode is not considered in the simulation. Nevertheless, it still can be found that the measured far-field scattering patterns are well consistent with simulated ones. This verifies that the user can control the scattering pattern of the RMCM prototype remotely with the his/her mind. It should be noted that with the increase of coding unit length, the split angle of the scattering pattern decreases gradually. This means a correspondence mapping can be established between the split angle and the user's attention intensity. Therefore, the RMCM also can be applied in attention monitoring, which is supplemented in the Additional file 1: Note S5. In addition, this mind-control framework can readily be applied to other scenarios such as mind-controlled fast switching among multiple functions. As a supplement, we also discuss the 2-bit coding case and present the scenario of mind-controlled fast switching among some typical functions of metasurfaces, which are supplemented in the Additional file 1: Note S6.

6 Conclusions

In this work, we propose a framework of achieving mind-controlled metasurfaces via brainwaves. The basic idea is to utilize the user's brainwaves to control the EM response of PMs. To achieve remote control, brainwaves signals are transmitted wirelessly from the user to the controller via Bluetooth. In this way, the EM response of metasurface can be mind-controlled remotely by a distant user. As an example, we demonstrated a RMCM which allows the user to control the scattering pattern under normal incidence. A brainwave extraction module is employed to extract the user's attention intensity signal, which is then used as the control signal of PMs. Both the simulated and test results show that the EM response of metasurface can be directly controlled by the user's brainwaves, with significantly improved control rate and switch rate. The RMCM shows good performances in EM wave modulation, providing a new route to intelligent metasurfaces. Our design provides users with a universal way to manipulate electromagnetic waves using brainwaves. Customized design for different users will further improve the accuracy of equipment in the future. Combined with intelligent algorithms such as machine learning, the intelligent process of the system will be further improved. This work can be readily extended to other mind-controlled functional or multi-functional metasurfaces and may find applications in health monitoring, 5G/6G communications, smart sensors, etc.

7 Methods

7.1 Numerical methods

The full-wave simulations of the metasurface are carried out using the time-domain solver in CST Microwave Studio 2019. The x-polarized plane waves are normally incident upon the metasurface from $+Z$ direction. The boundaries along x, y and z directions are set as open add space. Far-field monitor is set at 8.7 GHz to get the far-field scattering pattern. The development environment of Arduino is Arduino IDE version 1.8.8. The baud rate of signal transmission is set to 57,600 bit/s to ensure data transmission.

7.2 Samples fabrication

The metasurface is fabricated using conventional Printed Circuit Board (PCB) techniques. The PIN diodes is SMP1340-011 with SOD-323 packaging. And PIN diodes are soldered on the metasurface. A commercial microwave laminate F4B substrate with a dielectric constant $2.65(1+0.001\mathrm{j})$ is selected as the carrier to carry the structure. The size of meta-atom is 9×9 mm and the metasurface contains 30×30 meta-atoms. Considering the position of the biasing lines, the actual size of fabricated metasurface is 270×310 mm.

7.3 Measurement system

The far-field measurement is carried out in an anechoic chamber. The metasurface, together with the controller, is placed on the turntable mount. The two X-band antennas are set as transmitting and receiving terminals respectively. The transmitting antenna is placed along the normal of the metasurface while the receiving antenna can rotate around the metasurface, so as to measure the scattering patterns under normal incidence.

Supplementary Information

Additional file 1: Note S1. Modified equivalent circuit of PIN diodes via S-parameter measurement. **Note S2.** Biasing lines network. **Note S3.** Wearing mode of brainwave acquisition equipment. **Note S4.** Coding sequence display. **Note S5.** Application to attention monitoring. **Note S6.** Application to function-switching. **Figure S1.** Modification on the equivalent circuit of PIN diodes via measured data: **a** measurement setup; **b** modified equivalent circuit of the PIN diodes; **c** simulated reflectivity using the modified equivalent circuit; **d** simulated reflected phase using the modified equivalent circuit. **Figure S2.** Fabrication and design of metasurface: **a** metallized holes; **b** unit in the top layer; **c** middle metal reflection surface; **d** biasing lines in bottom layer. **Figure S3.** The wearing mode of brainwave acquisition equipment. **Figure S4.** Coding sequence display using LED array: **a** circuit design; **b**–**e** different coding sequences displayed by the LED array. **Figure S5.** Diagram of Attention detection applications. **Figure S6.** Application of the mind-control module to function switching.

Availability of data and materials
All data generated or analysed during this study are included in this published article and its Additional files.

Declarations

Competing interests
Cheng-Wei Qiu is an Editor for the journal, and no other author has reported any competing interests.

Author details
[1] Shaanxi Key Laboratory of Artificially-Structured Functional Materials and Devices, Air Force Engineering University, Xi'an 710051, Shaanxi, China. [2] National Key Laboratory of Science and Technology on Micro/Nano Fabrication, Department of Micro/Nano Electronics, Shanghai Jiao Tong University, Shanghai 200240, China. [3] Department of Electrical and Computer Engineering, Faculty of Engineering, National University of Singapore, 4 Engineering Drive 3, Singapore 117583, Singapore.

References
1. J. Xu, R. Yang, Y. Fan, Q. Fu, F. Zhang, A Review of tunable electromagnetic metamaterials with anisotropic liquid crystals. Front. Phys. **9**, 67 (2021)
2. Y. Liu, X. Zhang, Metamaterials: a new frontier of science and technology. Chem. Soc. Rev. **40**, 2494–2507 (2011)
3. X. Luo, Metamaterials and metasurfaces. Adv. Opt. Mater. **7**, 1900885 (2019)
4. D.R. Smith, J.B. Pendry, M.C. Wiltshire, Metamaterials and negative refractive index. Science **305**, 788–792 (2004)
5. S.A. Ramakrishna, Physics of negative refractive index materials. Reports Prog. Phys. **68**, 449–521 (2005)
6. N. Yu, F. Capasso, Flat optics with designer metasurfaces. Nat. Mater. **13**, 139–150 (2014)
7. S. Sun et al., Gradient-index meta-surfaces as a bridge linking propagating waves and surface waves. Nat. Mater. **11**, 426–431 (2012)
8. S. Sun, Q. He, J. Hao, S. Xiao, L. Zhou, Electromagnetic metasurfaces: physics and applications. Adv. Opt. Photon. **11**, 380–479 (2019)
9. X. Luo, Principles of electromagnetic waves in metasurfaces. Sci. China Phys. Mech. Astron. **58**, 594201 (2015)
10. S. Tang, T. Cai, H.-X. Xu, S. He, S. Sun, L. Zhou, Multifunctional metasurfaces based on the "merging" concept and anisotropic single-structure meta-atoms. Appl. Sci. (2018). https://doi.org/10.3390/app8040555
11. Y. Zhang, H. Liu, H. Cheng, J. Tian, S. Chen, Multidimensional manipulation of wave fields based on artificial microstructures. Optoelectron. Adv. **3**, 200002–200032 (2020)
12. M. Liu et al., Multifunctional metasurfaces enabled by simultaneous and independent control of phase and amplitude for orthogonal polarization states. Light Sci. Appl. **10**, 107 (2021)
13. D. Wen, S. Chen, F. Yue, K. Chan, M. Chen, M. Ardron et al., Metasurface device with helicity-dependent functionality. Adv. Opt. Mater. **4**, 321–327 (2016)
14. S. Boroviks, R.A. Deshpande, N.A. Mortensen, S.I. Bozhevolnyi, Multifunctional metamirror: polarization splitting and focusing. ACS Photonics **5**, 1648–1653 (2018)
15. B. Wang, F. Dong, Q.-T. Li, D. Yang, C. Sun, J. Chen et al., Visible-frequency dielectric metasurfaces for multiwavelength achromatic and highly dispersive holograms. Nano Lett. **16**, 5235–5240 (2016)
16. M.-X. Ren, W. Wu, W. Cai, B. Pi, X.-Z. Zhang, J.-J. Xu, Reconfigurable metasurfaces that enable light polarization control by light. Light Sci. Appl. **6**, e16254–e16254 (2017)
17. B. Zhu, Y. Feng, J. Zhao, C. Huang, T. Jiang, Switchable metamaterial reflector/absorber for different polarized electromagnetic waves. Appl. Phys. Lett. **97**, 51906 (2010)
18. Y.H. Fu, A.Q. Liu, W.M. Zhu, X.M. Zhang, D.P. Tsai, J.B. Zhang et al., A micromachined reconfigurable metamaterial via reconfiguration of asymmetric split-ring resonators. Adv. Funct. Mater. **21**, 3589–3594 (2011)
19. T. Driscoll, K. Hyun-Tak, C. Byung-Gyu, K. Bong-Jun, L. Yong-Wook, J.N. Marie et al., Memory metamaterials. Science **325**, 1518–1521 (2009)
20. T. Lewi, P.P. Iyer, N.A. Butakov, A.A. Mikhailovsky, J.A. Schuller, Widely tunable infrared antennas using free carrier refraction. Nano Lett. **15**, 8188–8193 (2015)
21. Q. Song et al., Water-resonator-based metasurface: an ultrabroadband and near-unity absorption. Adv. Opt. Mater. **5**, 1601103 (2017)
22. S. Cueff, Reconfigurable flat optics with programmable reflection amplitude using lithography-free phase-change material ultra-thin films. Adv. Opt. Mater. **9**, 2001291 (2021)
23. D.F. Sievenpiper, J.H. Schaffner, H.J. Song, R.Y. Loo, G. Tangonan, Two-dimensional beam steering using an electrically tunable impedance surface. IEEE Trans. Antennas Propag. **51**, 2713–2722 (2003)
24. H.-X. Xu et al., Dynamical control on helicity of electromagnetic waves by tunable metasurfaces. Sci. Rep. **6**, 27503 (2016)
25. J.Y. Dai et al., Wireless communications through a simplified architecture based on time-domain digital coding metasurface. Adv. Mater. Technol. **4**, 1900044 (2019)
26. N. Mou et al., Large-scale, low-cost, broadband and tunable perfect optical absorber based on phase-change material. Nanoscale **12**, 5374–5379 (2020)
27. A. Nemati et al., Ultra-high extinction-ratio light modulation by electrically tunable metasurface using dual epsilon-near-zero resonances. Opto-Electron Adv **4**, 200011–200088 (2021)
28. T.J. Cui, M.Q. Qi, X. Wan, J. Zhao, Q. Cheng, Coding metamaterials, digital metamaterials and programmable metamaterials. Light Sci. Appl. **3**, e218–e218 (2014)
29. X. Wan, M.Q. Qi, T.Y. Chen, T.J. Cui, Field-programmable beam reconfiguring based on digitally-controlled coding metasurface. Sci. Rep. **6**, 20663 (2016)
30. H. Yang, X. Cao, F. Yang, J. Gao, S. Xu, M. Li et al., A programmable metasurface with dynamic polarization, scattering and focusing control. Sci. Rep. **6**, 35692 (2016)
31. L. Li, T. Jun Cui, W. Ji, S. Liu, J. Ding, X. Wan et al., Electromagnetic reprogrammable coding-metasurface holograms. Nat. Commun. **8**, 197 (2017)
32. L. Zhang, X.Q. Chen, S. Liu, Q. Zhang, J. Zhao, J.Y. Dai et al., Space-time-coding digital metasurfaces. Nat. Commun. **9**, 4334 (2018)
33. Q. Yu, Y.N. Zheng, Z. Gu, J. Liu, Y.C. Liang, L.Z. Li et al., Self-adaptive metasurface platform based on computer vision. Opt. Lett. **46**, 3520–3523 (2021)
34. C. Qian, B. Zheng, Y. Shen, L. Jing, E. Li, L. Shen et al., Deep-learning-enabled self-adaptive microwave cloak without human intervention. Nat. Photonics **14**, 383–390 (2020)
35. Q. Ma, G.D. Bai, H.B. Jing, C. Yang, L. Li, T.J. Cui, Smart metasurface with self-adaptively reprogrammable functions. Light Sci. Appl. **8**, 98 (2019)

36. G.Y. Liu, L. Li, J.Q. Han, H.X. Liu, X.H. Gao, Y. Shi et al., Frequency-domain and spatial-domain reconfigurable metasurface. ACS Appl. Mater. Interfaces **12**, 23554–23564 (2020)

37. H. Xu, D.-F. Guan, B. Peng, Z. Liu, S. Yong, Y. Liu, Radar one-dimensional range profile dynamic jamming based on programmable metasurface. IEEE Antennas Wirel. Propag. Lett. **20**, 1883–1887 (2021)

38. Skyworks Solutions, SMP1340–011 Plastic Packaged PIN Diodes, https://www.rfmw.com/products/detail/smp1340011-skyworks/17809/. Accessed 11 Nov 2021

39. B. Stinson, D. Arthur, A novel EEG for alpha brain state training, neuro-biofeedback and behavior change. Complement. Ther. Clin. Pract. **19**, 114–118 (2013)

40. J.S. Kumar, P. Bhuvaneswari, Analysis of electroencephalography (EEG) signals and its categorization–a study. Procedia Eng. **38**, 2525–2536 (2012)

41. Q. Zheng et al., Wideband, wide-angle coding phase gradient metasurfaces based on Pancharatnam-Berry phase. Sci. Rep. **7**, 43543 (2017)

42. J.J. Yang, Y.Z. Cheng, D. Qi, R.Z. Gong, Study of energy scattering relation and RCS reduction characteristic of matrix-type coding metasurface. Appl. Sci. (2018). https://doi.org/10.3390/app8081231